AIRS Applications Technical Report

AIRS Drought Products for the United States Drought Monitor

Alireza Farahmand[1,2], Heidar Th. Thrastarson[2], Stephen J. Licata[2], Sharon Vasquez-Ray[2], Stephanie Granger[2]

[1] California State University Los Angeles
[2] Jet Propulsion Laboratory, California Institute of Technology

April 2025

Jet Propulsion Laboratory
California Institute of Technology
Pasadena, CA
Submit Questions to:
https://airs.jpl.nasa.gov/data/support/ask-airs

Table of Contents

The research was carried out at the Jet Propulsion Laboratory, California Institute of Technology, under a contract with the National Aeronautics and Space Administration (80NM0018D0004).

1. Introduction

The Atmospheric Infrared Sounder (AIRS) onboard NASA's Aqua satellite has been delivering measurements of atmospheric variables including temperature and humidity since its launch in 2002. Since 2016, the AIRS Project has delivered weekly application data products for the United States Drought Monitor (USDM), which is a drought monitoring system that takes into account drought indicators and information from a variety of sources to create standardized drought maps that are widely used by decision makers, policy experts, and researchers. This technical report documents the methodology and context of the AIRS drought products for the USDM.

The value of satellite data for drought monitoring and the literature relevant to AIRS and drought are introduced in the following subsections. In Section 2, the methodology to calculate drought indices is described and in Section 3, use cases are provided giving insight into the capability of AIRS data in identifying the precursor conditions of droughts. Section 4 covers the context of the collaboration between the AIRS Project and USDM authors and contains detailed descriptions of the AIRS drought products. Section 5 includes discussion of additional data products relevant for drought, the validation of the AIRS data products, and potential continuity of the drought products after the lifetime of the AIRS Mission.

1.1. Value of satellite data for drought monitoring

Droughts are catastrophic phenomena, which impact a wide variety of sectors including agriculture, vegetation health, and water resource management. The economic impacts of droughts are detrimental, with an estimated average annual economic loss of nearly six to eight billion dollars in the US, concentrated in agriculture (NCDC, 2019). Large scale droughts may result in extensive and severe impacts on food security (Haile, 2005). A major drought can reduce crop yields, lead farmers to cut back planted or harvested acreage, reduce livestock productivity, and increase costs of production inputs such as animal feed or irrigation water (USDA, 2013). According to the United Nations Convention to Combat Desertification (UNCCD), Over 1.4 billion people were affected by drought in the period of 2000 to 2019 and more than 10 million people lost their lives due to major drought events in the past century (UNCCD, 2022). Furthermore, droughts are the most destructive and costliest of natural disasters in developing regions. Eighty three percent of all economic losses from droughts in the developing countries were absorbed by agriculture between 2005 and 2015, with a price tag of $29 billion. While droughts occur globally, Africa as well as Latin America and the Caribbean are hit most by droughts, causing crop and livestock losses of $10.7 and $13 billion in those regions, respectively, between 2005 and 2015 (FAO, 2018).

Drought monitoring is challenging due to the complex nature of drought events. Droughts lack a single universal definition, which makes the drought monitoring and drought characterization difficult (Mishra & Singh, 2010). Since there is no single definition of droughts, they can be described in four main categories:

- *meteorological* drought is often described as a deficit in precipitation
- *agricultural* drought is expressed as a deficit in soil moisture
- *hydrological* drought typically refers to below average surface or sub-surface water
- *socioeconomic* drought pertains to water supply and social response (Wilhite, 2005)

Given that droughts can be described relative to different variables, numerous indices based on precipitation, soil moisture, surface and groundwater, and vegetation health have been developed based on one or more climatic variables (Wilhite, 2000). Some examples include Standardized Precipitation Index (SPI, McKee et al., 1993), Palmer Drought Severity Index (PDSI, Wells et al., 2004), Evaporative Stress Index (ESI, Anderson et al., 2007), Standardized Precipitation Evapotranspiration Index (SPEI, Vicente-Serrano et al., 2010), Standardized Vegetation Index (SVI, Peters et al., 2002) and Multivariate Standardized Drought Index (MSDI, Hao and AghaKouchak, 2013).

Traditionally, droughts have been monitored by ground-based observation. However, limitations in ground-based observations including uneven distribution of ground-based observations, temporal and spatial inconsistencies, and lack of observations in remote regions have made satellite observations a great asset for drought monitoring. The advantages of remote sensing data in drought monitoring are the large spatial coverage and high temporal frequency of the observations, which leads to a better understanding of the spatial extent of drought and its duration, and improved detection of the onset of drought and its intensity (AghaKouchak et al., 2015). For example, Land Surface Temperature (LST) observations from Thermal Infrared (TIR) satellite imagery have been widely used for drought monitoring. Some of the TIR-based indices are Temperature Conditions Index (TCI; Kogan, 1995)), Vegetation Health Index (VHI; Kogan, 1995) and Evaporative Stress Index (ESI, Anderson et al., 2007).

1.2. Drought early detection

To mitigate the impact of drought on human life and environment and to ensure the production of adequate food to avoid food crises, developing early warning and mitigation strategies is critical. Drought early onset detection is fundamental to local and regional mitigation plans, especially in the agriculture and water resources sectors. A water manager may need drought information months in advance for water resource planning, while for a farmer even a few weeks of lead time is game changing. Early detection, even

by a few weeks/months, allows farmers to take adaptive measures that include purchasing less fertilizer and increasing insurance coverage, especially before or early in the growing season.

1.3. AIRS publications on drought

Recent studies indicate that drought indicators based on air Relative Humidity (*RH*), air Temperature (*T*), and air Vapor Pressure Deficit (*VPD*), derived from the Atmospheric Infrared Sounder (AIRS) mission can detect the onset of droughts earlier than other drought indicators, specifically *SPI* which is widely used for drought onset detection.

Relative humidity is an important climate variable defined as the ratio of air vapor pressure to the saturated vapor pressure. Precipitation and relative humidity are related to each other in the sense that precipitation is not expected at low relative humidity. Farahmand et al. (2015) showed that Standardized Relative Humidity Index (*SRHI*) can detect drought signals earlier than the precipitation-based *SPI*. Specifically, they show the probability of drought onset (DO) detection (i.e., fraction of detected drought) using *SRHI* when $DO_{SRHI} \leq DO_{SPI}$ ranges globally between 0.5 to 0.8, with the global average being approximately 0.6 (i.e., 60% of all events). This study also indicates that the mean lead time of *SRHI* relative to *SPI* ranges between 1 to 3 months with the global average being approximately 1.9 months. The study further shows that *SRHI* has been able to successfully detect the early signs of the 2012 Midwest drought, the 2011 Texas drought, and the 2010 Russian Drought.

In another study, Standardized Vapor Pressure Deficit (*SVPD*) and Standardized Temperature (*ST*) indicators were shown to detect droughts earlier or at the same time as *SPI* with an average relative lead time of 1.5 months (a range of a few weeks to 2 months) and in 60 percent of events in the Contiguous United States (CONUS) (Behrangi et al., 2016). Vapor Pressure Deficit (*VPD*), defined as the difference between vapor pressure and saturated vapor pressure, is an important climate variable, which includes both elements of temperature and relative humidity. *VPD* is a major controlling factor of evapotranspiration demand. With increasing air aridity, *VPD* increases, indicating greater evaporation stresses (Behrangi et al., 2015; Kucera, 1954).

Behrangi et al. (2015) found that the combination of high temperatures and low atmospheric humidity, which was expressed by high *VPD*, were important factors in the development and evolution of both the 2011 and 2012 droughts in the South central and Corn Belt regions of the United States. The *SVPD* indicated increases during the formation and rapid intensification in drought conditions of the 2011 and 2012 drought

events, suggesting that remotely sensed *VPD* holds considerable potential to offer new atmospheric insights for drought early warning and assessment.

2. Methodology for calculating the *RH, T, VPD* drought indices

Standardized drought indicators based on *RH, T, and VPD* can be derived using either a parametric or a non-parametric approach. The non-parametric (empirical) approach helps avoid assumptions about the underlying distribution functions (Farahmand and AghaKouchak, 2015). In this section, the methodology for deriving *SVPD* is explained. *SRHI* and *ST* indicators are calculated using a similar methodology. To derive *SVPD*, *VPD* should first be calculated. *VPD* is defined as the difference between vapor pressure (e) and saturated vapor pressure (es) and calculated as:

$$VPD = c1 \times \exp\left(\frac{c2 \times T}{c3 + T}\right) - c1 \times \exp\left(\frac{c2 \times Td}{c3 + Td}\right)$$

(Equation 1)

where c1=0.611 kPa, c2=17.5, c3= 240.978 °C, Td: dew point temperature (°C), T: air temperature (°C).

Td is calculated from *T* and *RH*:

$$Td = \frac{c \times \alpha(T, RH)}{b - \alpha(T, RH)}$$

(Equation 2)

$$\alpha(T, RH) = \ln\left(\frac{RH}{100}\right) + \frac{(b \times T)}{(c + T)}$$

(Equation 3)

where *b* = 17.625 and *c* =243.04 °C.

The empirical *SVPD* can then be derived by first calculating the marginal probabilities of *VPD* (Gringorten, 1963):

$$p(x_i) = \frac{i-0.44}{n+0.12}$$

(Equation 4)

Here *n* is the sample size, *i* denotes the rank of non-zero *VPD* data from the smallest, and $p(x_i)$ is the corresponding empirical marginal probability. *SVPD* is then derived using the following equation:

$$SVPD = \phi^{-1}(p)$$

(Equation 5)

where $\boldsymbol{\phi}$ is the standard normal distribution function, and *p* is probability derived from Equation 4. *SRHI* and *ST* can be calculated following a similar methodology.

To facilitate comparing these indices with other available drought indicators such as *SPI*, the signs of *SVPD* and *ST* are reversed so that negative *SVPD* and *ST* indicates above average vapor pressure deficit and temperature respectively and is proposed as a measure of dryness. Positive *SVPD* and *ST* indicates below average vapor pressure deficit and temperature and is proposed as a measure of wetness (Behrangi et al., 2015, 2016). One attractive feature of *SVPD*, *SRHI*, and *ST* is that, similar to *SPI*, they can be derived for different timescales (e.g., 1-, 3-, 6-month *SVPD*). For further information about deriving *SRHI*, *SVPD*, and *ST* indices, please refer to Behrangi et al. (2015, 2016) and Farahmand et al. (2015).

3. Use cases

In this section, AIRS drought indicators are compared to MERRA2 (Modern-Era Retrospective analysis for Research and Applications) *SPI* and *SSI* (Standardized Soil Moisture Index) for drought onset detection in three case studies (Farahmand et al., 2023) (Figure 1). MERRA2 provides re-analysis precipitation and soil moisture data at the resolution of 0.625° longitude by 0.5° latitude since 1980 (Gelaro et al. 2017). We use the moderate drought threshold of 20th percentile and various smoothing scales depending on the type of drought. For simplicity, we only showcase AIRS *VPD* drought indicator (*SVPD*) results in this report.

3.1. Use Case 1: 2012 Midwest Flash Drought

Figure 1a shows the development of the 2012 Midwestern Flash Drought based on two-month indicators of *SVPD2*, *SPI2*, and *SSI2*. The blue line indicates *SVPD2*, the red line indicates *SPI2*, and the yellow line indicates *SSI2*. As indicated, *VPD* showed the onset of drought several months earlier than precipitation and soil moisture. Precipitation showed the drought signals in May 2012. Soil Moisture did not show drought conditions until June 2012. For this event, AIRS *VPD* data picked up a drought signal that might otherwise have been overlooked by precipitation and soil moisture.

3.2. Use Case 2: 2019 Southeast Flash Drought

In Figure 1b, the development of the 2019 Southeastern Flash Drought is shown. This event developed rapidly during Fall 2019. Due to rapid development, we assessed the drought development using 1-month drought indicators of *VPD* (*SVPD1*), precipitation (*SPI1*), and soil moisture (*SSI1*). As shown, the drought onset was simultaneously captured by all three indicators of *SVPD*, *SPI*, and *SSI*. In this case study of a very abrupt flash drought, the *SVPD1*, *SPI1*, and *SSI1* signals all began at the same time.

3.3. Use Case 3: 2020-2022 Western US Drought

Figure 1c shows the development of the 2020-2022 Western U.S. Drought. To investigate this event, we looked at the 3-month drought indicators (*SVPD3*, *SPI3*, and *SSI3*), as this event was not considered a flash drought. As shown, the drought onset was simultaneously captured by all indicators. Although this event was not a flash drought, AIRS-based drought indicators along with drought indicators of precipitation and soil moisture were able to detect the drought onset. The results of these case studies have provided insight into the capability of AIRS data in identifying the precursor conditions of droughts, particularly in the case of flash droughts.

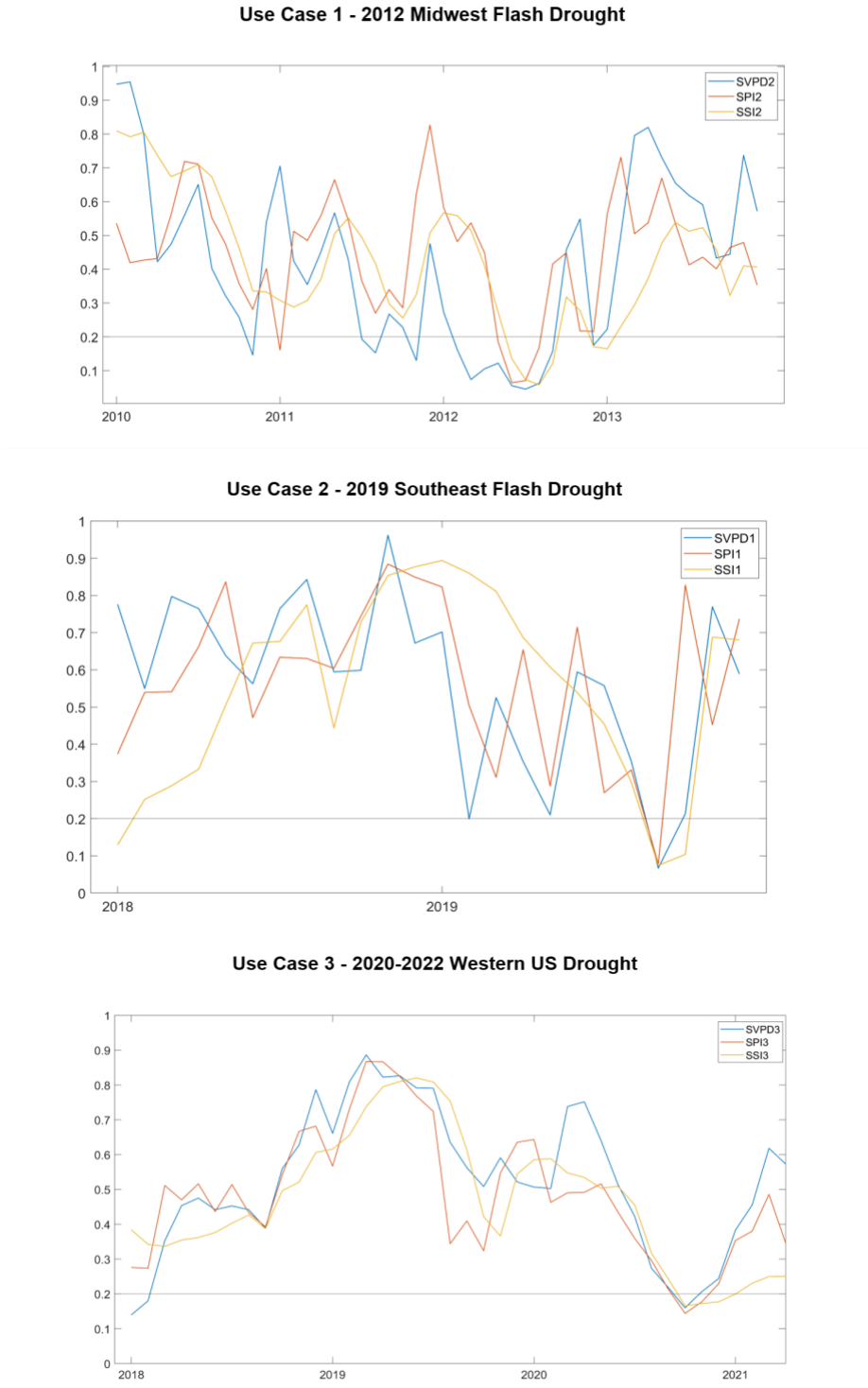

Figure 1. Assessment of drought onset for three case studies of a) 2012 Midwestern flash drought; 2) 2019 Southeastern flash drought; 3) 2020-2022 Western US drought. SVPD indicators are based on AIRS data. SPI and SSI are precipitation and soil moisture indicators, respectively, based on MERRA reanalyses. The appended numbers in the legend indicate averaging times in months.

4. AIRS and USDM

4.1. History of AIRS and USDM

The United States Drought Monitor (USDM) framework is a drought monitoring system that considers several variables including short- and long-term drought indicators, vegetation information, hydrologic indices, and remote-sensing information, along with the ground validation to create weekly drought maps. The USDM authors combine the objective drought indicators and the subjective inputs of local and regional experts such as state climatologists, National Weather Service staff, Extension agents, and hydrologists to synthesize the best available data and manually create weekly drought depictions for the United States. The USDM maps are generally at the spatial resolution of counties. The USDM maps are available since 1999 and show areas of the United States under drought in six classifications: No drought, D0 (Abnormally Dry), D1 (Moderate Drought), D2 (Severe Drought), D3 (Extreme Drought), and D4 (Exceptional Drought) (Svoboda et al. 2002).

Policymakers routinely use the USDM to help determine drought relief allocations and declarations of drought. The integrated approach makes the USDM one of the most holistic measures of drought conditions across the United States, Puerto Rico, U.S. Virgin Islands, and U.S. Affiliated Pacific Islands. In addition, USDM maps are widely used in a variety of ways including academic research, informing decision makers and policy experts, aiding in the declaration of drought disaster areas, and delivering billions of dollars in economic assistance to agricultural communities through the Livestock Forage Disaster Program (LFP).

Given the value of AIRS drought products in detecting drought onset, the AIRS drought team initiated a conversation with the National Drought Mitigation Center (NDMC) in early 2016 to explore the possibility of integrating AIRS drought products into the USDM process. The AIRS drought team later visited the NDMC at the University of Nebraska Lincoln (UNL) in the Spring of 2016 and showcased the value of AIRS near surface *RH*, *T*, and *VPD* drought products in detecting drought onset. NDMC agreed to evaluate and potentially utilize AIRS drought products in generating weekly drought maps.

4.2. AIRS Drought Products for USDM

Each week (since mid-2017), the AIRS Project has made available for download by the USDM community a standard set of CONUS daytime drought products for three key parameters: Surface Relative Humidity (*RH*), Surface Air Temperature (*T*), and Surface Vapor Pressure Deficit (*VPD*). Each of the AIRS *RH, T, and VPD* drought products are

binned into four timescales of 7, 14, 28, and 56-day averages resulting in a total of 12 drought products that can be utilized to help with drought assessment. These data points are at the spatial resolution of half-degree. The inputs for generating drought maps are Level 2 AIRS observations (50 km resolution at nadir) made from AIRS IR-Only processing rules which do not incorporate observations from AIRS' sister instrument, the Advanced Microwave Sounder Unit-A. All twelve drought products are formatted specifically for use by USDM authors including a specific type of projection, data format, and color bar. All data have been staged at the publicly accessible NASA JPL server and pulled by NDMC every Monday since April 2017. In 2020, the AIRS project added an "integrity" check before delivering all products to ensure maps follow the requirements set by USDM. It is important to note the AIRS drought products are derived from direct satellite observations, which add another remotely sensed tool to the suite of satellite products being utilized in the weekly USDM assessment.

4.3. Methodology for USDM drought indices

All drought products are derived from daily AIRS Version 7 Level 2 Hierarchical Data Format (HDF) data files. Level 2 data are organized according to a satellite swath path at 50 km resolution but are not gridded. The first two parameters exist as data fields in the delivered data products:

1. Surface Air Temperature (*TSurfAir*)

2. Surface Relative Humidity (*RelHumSurf*)

A calculation is then performed to generate surface dew point temperature (*Td*) from *TSurfAir* and *RelHumSurf* using equations 2 and 3.

3. Vapor Pressure Deficit (*VPD*)

Td enables the calculation of the third parameter Vapor Pressure Deficit (*VPD*) from *TSurfAir* and *Td* using equation 1.

The AIRS Level 2 data extracted are only from ascending node orbital ground tracks which, for the latitude range of the continental United States (CONUS), always correspond to daylight conditions.

4.3.1. Data Quality Constraints

The AIRS Version 7 Level 2 observation set provides several types of quality control (QC) parameters associated with each vertical atmospheric profile. Each of these QC

parameters is assigned a value as follows: 0= best; 1=Good; 2=Suspect. The following seven QC parameters are extracted in the process of creating the AIRS drought products:

1. TSurfAir_QC: Surface Air Temperature

2. RelHumSurf_QC: Surface Relative Humidity Quality Control

3. CldFrcTota_QC: Total Cloud Fraction Quality Control

4. PSurfStd_QC: Surface Skin Pressure Quality Control

5. TSurfStd_QC: Surface Skin Temperature Quality Control

6. PTropopause_QC: Tropopause Pressure Quality Control

7. T_Tropopause_QC: Tropopause Temperature Quality Control

As originally implemented, the AIRS drought products would exclude any Level 2 atmospheric profile in which any of the above seven QC parameters had a value of “2” (suspect). However, a follow-up analysis revealed that a significant number of profiles were being excluded for the reason of just one QC Indicator; namely TSurfStd_QC. Further studies revealed that the evaluation of TSurfStd_QC included a more rigorous convergence criteria which was more suited to an ocean surface, where the emissivity generally has less uncertainty than over land. As a result, the current AIRS drought product no longer includes TSurfStd_QC as a disqualifying parameter.

4.3.2. Data Aggregation Approach

After applying the above (six-parameter) QC filtering tests, the remaining profiles for each daily data set (ascending node/daylight conditions only) are averaged into a latitude-longitude box measuring one-half degree on a side. This one-half-degree box then becomes the basic unit for subsequent drought parameter calculation for *TSurfAir*, *RelHumSurf* and *VPD*.

4.3.3. Specific calculation of the percentile

The procedure used to calculate percentile ranks over a given time scale is illustrated below by examining a specific example for the 7-day average Surface Air Temperature for June 27, 2021.

To derive drought conditions, we calculate the percentile rank of the most recent 7, 14, 28, and 56-day periods for these parameters, within the context of those same calendar date ranges from the AIRS science data record going back to September 1, 2002. To that

end, the Gringorten method (Equation 4) is applied (Farahmand et al. 2015; Behrangi et al. 2016). Let's assume we would like to derive AIRS Surface Air Temperature (*TSurfAir*) percentiles for the 7-day period ending on June 27, 2021. The target period should be compared against the data collection of the same time period from the years of 2003, 2004, 2005 … up to and including 2021.

Note that this comparison only represents a set of 19 data points (i.e., the same 7-day averages from 19 consecutive years). To enable a more realistic calculation of percentile, (i.e. about 100 data points), it is necessary to add additional data points to the background data set, even if not all of these could be independent of each other.

The remainder of the data set is composed of seven additional sliding date windows from each of the reference years. For example, the 2003-2021 data collection contains the following 7-day periods for which averaged TSurfAir values are obtained, for a total of 152 data points [19 years x 8 seven-day averages]:

June 21- 27, June 20-26, June 19-25, June 18-24, June 17-23, June 16-22, June 15-21, June 14-20 [2021]

June 21- 27, June 20-26, June 19-25, June 18-24, June 17-23, June 16-22, June 15-21, June 14-20 [2020]

June 21- 27, June 20-26, June 19-25, June 18-24, June 17-23, June 16-22, June 15-21, June 14-20 [2019]

…..

June 21- 27, June 20-26, June 19-25, June 18-24, June 17-23, June 16-22, June 15-21, June 14-20 [2004]

June 21- 27, June 20-26, June 19-25, June 18-24, June 17-23, June 16-22, June 15-21, June 14-20 [2003]

The result is a large, pseudo-independent data set that reveals changes to 7-day averages on a smaller time scale (the sliding data window). Therefore, the percentile calculation of TSurfAir in the 7-day drought period is the comparison of the 7-day average value (June 21-27, 2021) against the data set of all the above data points (152 7-day periods, 2003-2021).

A similar approach is used for deriving drought indicators of 14-day, 28-day and 56-day time scales.

4.4. Sample USDM drought product

For each drought parameter and each of the four date range categories, two GeoTiff data files are produced. The first GeoTiff shows for each half-degree lat/lon box its ranking (0 – 100) in which the lower values represent stronger drought conditions. The second GeoTiff shows for each half-degree lat/lon box an RGB triplet value (0-255) that translates the percentile rank into a specific color, as shown in Figures 2-4. The final integrated USDM drought map highlights AIRS data from the following drought regimes:

D0: Abnormally dry (yellow)

D1: Moderate drought (tan)

D2: Severe drought (orange)

D3: Extreme drought (red)

D4: Exceptional drought (brown)

Specifically, Figures 2-4 show the RGB rendering of the drought percentile ranking, for the 7-day period ending June 29, 2021, for the Surface Air Temperature, Surface Relative Humidity and Vapor Pressure Deficit, against a climatology based on that same calendar date range from each year going back to June 2003, as described above in Secion 4.3.3. White regions are within historical norms (a wide range of percentile values), blue areas are cooler and wetter than normal, and black squares represent data that has been excluded by a comprehensive set of AIRS quality control (QC) parameters. All large water bodies including The Great Lakes and The Great Salt Lake are also excluded from analysis and are shown as black squares.

In Figure 2 (Surface Air Temperature), note that even in the context of a 19-year climatology, a well-publicized heat wave in the Pacific Northwest ranked in the upper 1 percent (brown) of surface air temperatures. Figures 3 and 4 illustrate similar anomalous conditions from this same 7-day period in 2021 for Surface Relative Humidity and Vapor Pressure Deficit respectively. In particular, the *VPD* plot seems to have captured the drought signal of both surface temperature and relative humidity.

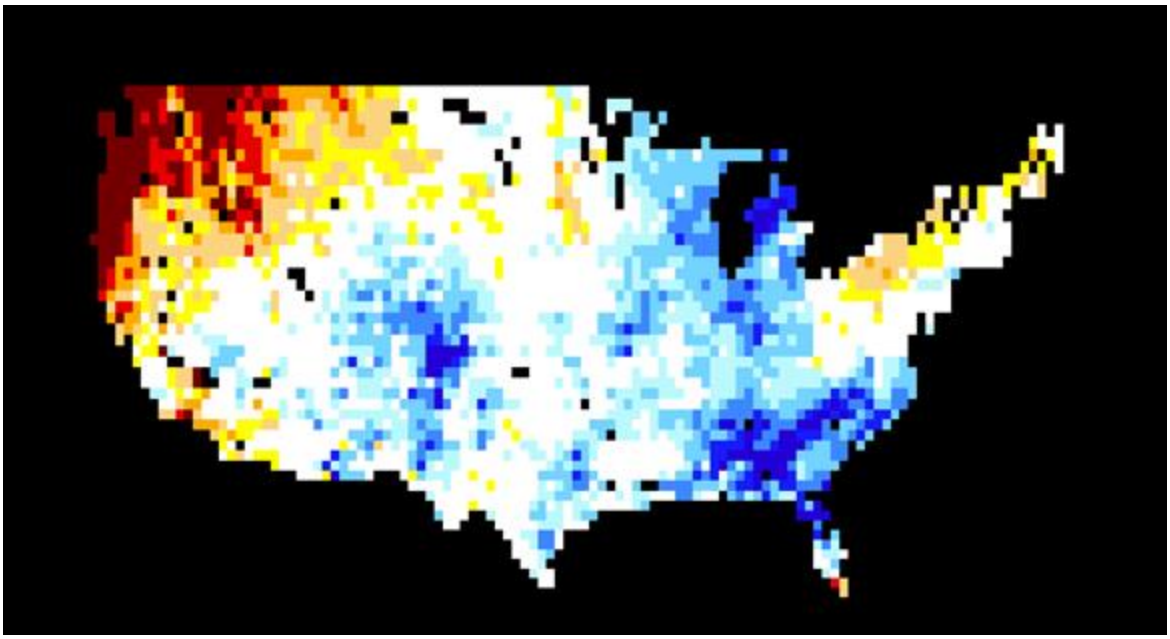

Figure 2. Anomaly plot of 7-day-averaged CONUS Surface Air Temperature for June 23-29, 2021.

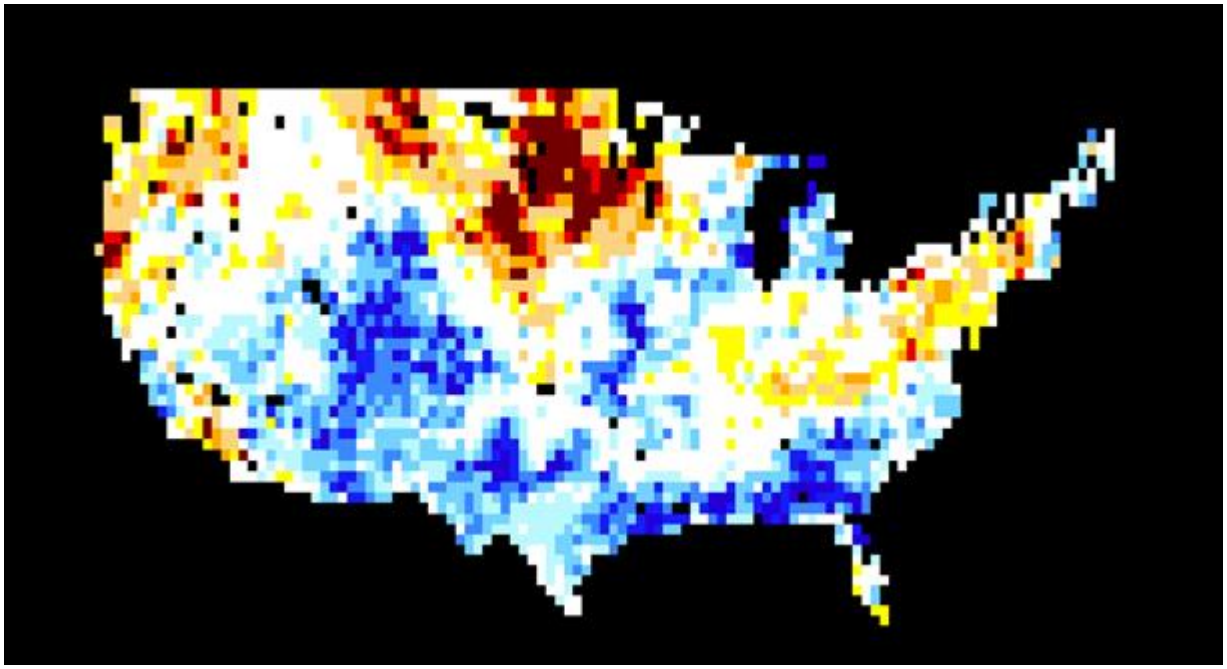

Figure 3. Anomaly plot of 7-day-averaged CONUS Surface Relative Humidity for June 23-29, 2021.

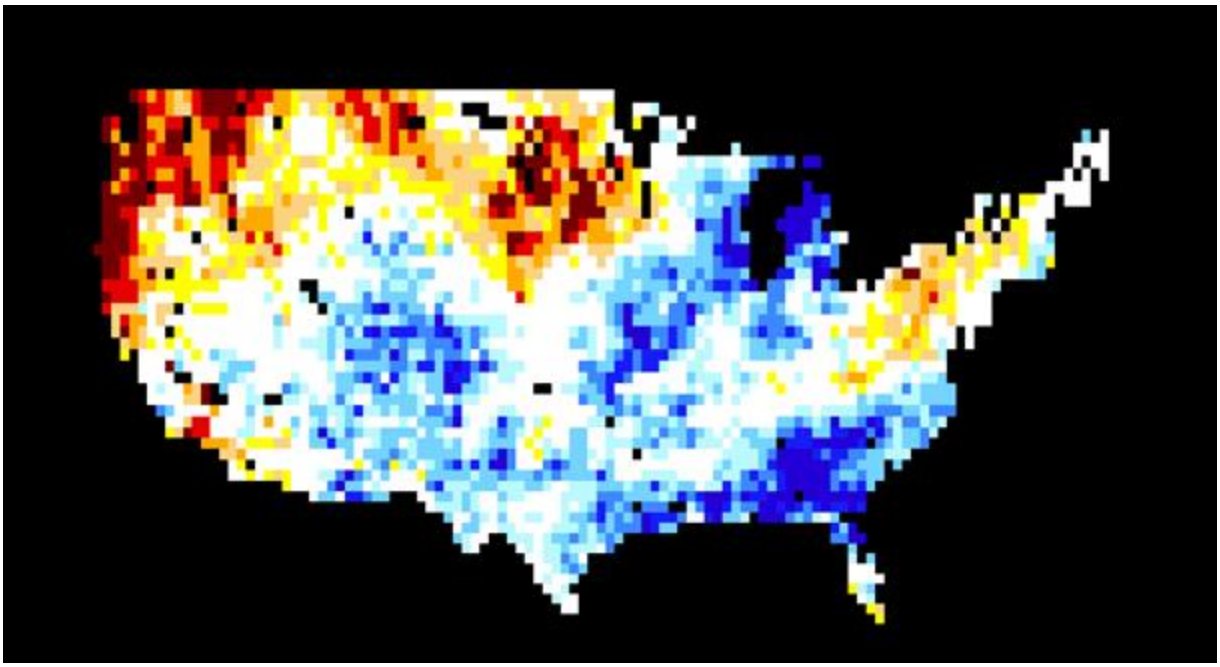

Figure 4. Anomaly plot of 7-day-averaged CONUS Vapor Pressure Deficit for June 23-29, 2021.

Following from the description above, the AIRS drought products released each Monday consist of 24 data products: A pair of GeoTiff files (percentile rank and RGB color codes) for the three drought parameters (Surface Air Temperature, Surface Relative Humidity, and Vapor Pressure Deficit) as they are historically ranked over four time-intervals ending the same date as previous 7, 14, 28 and 56-day periods).

These GeoTiff files follow the filename convention illustrated by the following example for the June 14, 2021:

RelHumSurfPctile_conus_Asc_IROnly_14dwin_20210614.tif
RelHumSurfPctile_3drgb_conus_Asc_IROnly_14dwin_20210614.tif

RelHumSurfPctile_conus_Asc_IROnly_28dwin_20210614.tif
RelHumSurfPctile_3drgb_conus_Asc_IROnly_28dwin_20210614.tif

RelHumSurfPctile_conus_Asc_IROnly_56dwin_20210614.tif
RelHumSurfPctile_3drgb_conus_Asc_IROnly_56dwin_20210614.tif

RelHumSurfPctile_conus_Asc_IROnly_7dwin_20210614.tif
RelHumSurfPctile_3drgb_conus_Asc_IROnly_7dwin_20210614.tif

VPDPctile_conus_Asc_IROnly_14dwin_20210614.tif
VPDPctile_3drgb_conus_Asc_IROnly_14dwin_20210614.tif

VPDPctile_conus_Asc_IROnly_28dwin_20210614.tif
VPDPctile_3drgb_conus_Asc_IROnly_28dwin_20210614.tif

VPDPctile_conus_Asc_IROnly_56dwin_20210614.tif
VPDPctile_3drgb_conus_Asc_IROnly_56dwin_20210614.tif

VPDPctile_conus_Asc_IROnly_7dwin_20210614.tif
VPDPctile_3drgb_conus_Asc_IROnly_7dwin_20210614.tif

TSurfAirPctile_conus_Asc_IROnly_14dwin_20210614.tif
TSurfAirPctile_3drgb_conus_Asc_IROnly_14dwin_20210614.tif

TSurfAirPctile_conus_Asc_IROnly_28dwin_20210614.tif
TSurfAir_Pctile_3drgb_conus_Asc_IROnly_28dwin_20210614.tif

TSurfAirPctile_conus_Asc_IROnly_56dwin_20210614.tif
TSurfAirPctile_3drgb_conus_Asc_IROnly_56dwin_20210614.tif

TSurfAirPctile_conus_Asc_IROnly_7dwin_20210614.tif
TSurfAirPctile_3drgb_conus_Asc_IROnly_7dwin_20210614.tif

5. AIRS Data, Validation and Continuity

5.1. Validation

AIRS drought products for near-surface temperature, relative humidity and *VPD* are delivered weekly to the USDM (see Section 2 and 4). The AIRS drought products are derived from data products that are validated as part of the general AIRS data validation strategy. AIRS processing software is updated every three to five years and the entire mission data set is reprocessed using the new version. All key variables are validated and compared with independent datasets such as from ground-based stations, other satellites and reanalysis datasets. Results are published in validation and testing reports. The AIRS Level 2 near-surface air temperature and relative humidity data that is used to produce the AIRS drought products released to the USDM are validated as part of this process.

The latest test report published with the release of AIRS Version 7 (Yue et al., 2020) includes analysis of temperature, relative humidity, and *VPD*, specifically in the context of drought. It is based on the two latest versions of AIRS data, Versions 6 and 7, and focuses on the case of the 2011 major drought in Texas. In summary, both Version 6 and 7 are found to capture anomaly locations and time series in the 2011 Texas drought.

5.2. AIRS Version 7 VPD data

The latest version of AIRS data available to the public is Version 7. In this version, a global, daily *VPD* product is included as a Level 2 product. This is data that is organized according to the satellite swath path at around 45 km horizontal resolution but is not gridded. The same equations are used to calculate the *VPD* as are used in AIRS products for USDM (see Section 2). Quality indicators are included for each *VPD* data point, but no comparison to the long-term data record is included and the data are not processed to be reported as percentiles as described in Section 4. However, all the data needed to create a long-term record for temperature, humidity and *VPD* is available from 2002 up to the present.

5.3. Data continuity

The AIRS instrument is expected to cease operations in the near future, but similar sounder data will continue to be available from other satellites. The Cross-track Infrared Sounder (CrIS) instrument will continue delivering similar capability, also paired with the Advanced Technology Microwave Sounder (ATMS). The CrIS and ATMS instruments

onboard the Joint Polar Satellite System (JPSS) have yielded global atmospheric temperature, pressure and moisture profiles from space since 2011. Drought products such as the AIRS products delivered to the USDM are not currently produced from CrIS/ATMS data but can be derived with the same principles.

References

AghaKouchak, A., Farahmand, A., Melton, F. S., Teixeira, J., Anderson, M. C., Wardlow, B. D., & Hain, C. R. (2015). Remote sensing of drought: Progress, challenges and opportunities. *Reviews of Geophysics, 53*(2), 452–480. https://doi.org/10.1002/2014RG000456

Anderson, M. C., Norman, J. M., Mecikalski, J. R., Otkin, J. A., & Kustas, W. P. (2007). A climatological study of evapotranspiration and moisture stress across the continental United States based on thermal remote sensing: 2. Surface moisture climatology. *Journal of Geophysical Research*, *112*(D11). https://doi.org/10.1029/2006JD007507

Behrangi, A., Loikith, P., Fetzer, E., Nguyen, H., & Granger, S. (2015). Utilizing Humidity and Temperature Data to Advance Monitoring and Prediction of Meteorological Drought. *Climate*, *3*(4), 999–1017. https://doi.org/10.3390/cli3040999

Behrangi, A., Fetzer, E. J., & Granger, S. L. (2016). Early detection of drought onset using near surface temperature and humidity observed from space. *International Journal of Remote Sensing*, *37*(16), 3911–3923. https://doi.org/10.1080/01431161.2016.1204478

FAO. (2018, March 15). Disasters causing billions in agricultural losses, with drought leading the way. Retrieved from http://www.fao.org/news/story/en/item/1106977/icode/

UNCCD. (2022). DROUGHT IN NUMBERS 2022- restoration for readiness and resilience -Retrieved from https://www.unccd.int/resources/publications/drought-numbers

Farahmand, A., AghaKouchak, A., & Teixeira, J. (2015). A Vantage from Space Can Detect Earlier Drought Onset: An Approach Using Relative Humidity. *Scientific Reports*, *5*(1). https://doi.org/10.1038/srep08553

Farahmand, A., Ray, S., Thrastarson, H., Licata, S., Granger, S., & Fuchs, B. (2023). A Workshop on Using NASA AIRS Data to Monitor Drought for the U.S. Drought Monitor. *Bulletin of the American Meteorological Society, 104*(1), E22–E30. https://doi.org/10.1175/BAMS-D-22-0222.1

Gelaro, R., McCarty, W., Suárez, M. J., Todling, R., Molod, A., Takacs, L., et al. (2017). The Modern-Era Retrospective Analysis for Research and Applications, Version 2 (MERRA-2). *Journal of Climate*, *30*(14), 5419–5454. https://doi.org/10.1175/JCLI-D-16-0758.1

Gringorten, I. I. (1963). A plotting rule for extreme probability paper. *Journal of Geophysical Research*, *68*(3), 813–814. https://doi.org/10.1029/JZ068i003p00813

Haile, M. (2005). Weather patterns, food security and humanitarian response in sub-Saharan Africa. *Philosophical Transactions of the Royal Society B: Biological Sciences*, *360*(1463), 2169–2182. https://doi.org/10.1098/rstb.2005.1746

Hao, Z., & AghaKouchak, A. (2013). Multivariate Standardized Drought Index: A parametric multi-index model. *Advances in Water Resources*, *57*, 12–18. https://doi.org/10.1016/j.advwatres.2013.03.009

Kogan, F. N. (1995). Application of vegetation index and brightness temperature for drought detection. *Advances in Space Research*, *15*(11), 91–100. https://doi.org/10.1016/0273-1177(95)00079-T

Kucera, C. L. (1954). Some relationships of evaporation rate to vapor pressure deficit and low wind velocity. *Ecology*, *35*(1), 71–75.

McKee, T., Doesken, N., & Kleist, J. (1993). The relationship of drought frequency and duration to time scales. *Proceedings of the 8th Conference on Applied Climatology*, *17*(22), 179–183.

Mishra, A. K., & Singh, V. P. (2010). A review of drought concepts. *Journal of Hydrology*, *391*(1–2), 202–216. https://doi.org/10.1016/j.jhydrol.2010.07.012

NCDC. (2019). DROUGHT: Monitoring Economic, Environmental, and Social Impacts. Retrieved from https://www.ncdc.noaa.gov/news/drought-monitoring-economic-environmental-and-social-impacts

Peters, A. J., Walter-Shea, E. A., Ji, L., Vina, A., Hayes, M., & Svoboda, M. (2002). Drought monitoring with NDVI-based standardized vegetation index. *Photogrammetric Engineering and Remote Sensing, 68*, 71–75.

Vicente-Serrano, S. M., Beguería, S., & López-Moreno, J. I. (2010). A Multiscalar Drought Index Sensitive to Global Warming: The Standardized Precipitation Evapotranspiration Index. *Journal of Climate*, *23*(7), 1696–1718. https://doi.org/10.1175/2009JCLI2909.1

Wells, N., Goddard, S., & Hayes, M. J. (2004). A Self-Calibrating Palmer Drought Severity Index. *Journal of Climate*, *17*(12), 2335–2351. https://doi.org/10.1175/1520-0442(2004)017<2335:ASPDSI>2.0.CO;2

Wilhite, D. A. (2000). Drought: A global assessment. Routledge.

Wilhite, D. A. (2005). Drought and Water Crises: Science, Technology, and Management Issues (Vol. 86, p. 432). CRC Press.

Yue, Q., Lambrigtsen, B. (Eds.), Blaisdell, J. M., Farahmand, A., Fetzer, E. J., Fishbein, E., Griffin, E., Iredell, L., Irion, F. W., Kahn, B. H., Kalmus, P., Manning, E., Marchetti, Y., Pagano, T., Smith, N., Susskind, J., Teixeira, J., Thrastarson, H. T., Wang, T., Wen, Y., Wilson, R. C., and Wong, S. (2020). AIRS Version 7 Level 2 Performance Test and Validation Report. Jet Propulsion Laboratory, California Institute of Technology, Pasadena, CA. https://docserver.gesdisc.eosdis.nasa.gov/public/project/AIRS/V7_L2_Performance_Test_and_Validation_report.pdf